

Three-phase DC/AC power converter with power quality optimization

Convertidor DC/AC trifásica con optimización de la calidad de la energía

DOI: <http://doi.org/10.17981/ingecuc.18.1.2022.20>

Artículo de Investigación Científica. Fecha de Recepción: 18/03/2022. Fecha de Aceptación: 27/04/2022.

Jorge Luis Díaz Rodríguez 

Universidad de Pamplona. Pamplona (Colombia)
jdiazcu@unipamplona.edu.co

Luis David Pavón Fernández 

Universidad de Pamplona. Pamplona (Colombia)
martincepeda08@gmail.com

Edison Andrés Caicedo Peñaranda 

Universidad de Pamplona. Pamplona (Colombia)
edison.caicedo@unipamplona.edu.co

To cite this paper

J. Díaz Rodríguez, L. Pavón Fernández & E. Caicedo Peñaranda, “Three-phase DC/AC power converter with power quality optimization,” *INGE CUC*, vol. 18, no. 1, pp. 277–290. DOI: <http://doi.org/10.17981/ingecuc.18.1.2022.20>

Resumen

Introducción— Los sistemas de conversión DC/AC utilizados actualmente en múltiples aplicaciones como las fuentes alternativas de energía involucra problemas de la calidad de la energía debido regulaciones de tensión y deformaciones como las causadas por la distorsión armónica.

Objetivo— Desarrollar un prototipo que a través de un algoritmo genético multiobjetivo permita optimizar la calidad de la energía de los sistemas de inversión trifásicos a través del uso de convertidores multinivel.

Metodología— Se define el prototipo a utilizar en la conversión de potencia, se modela matemáticamente la tensión de salida, se desarrollan los algoritmos genéticos multiobjetivo de optimización, se implementa el prototipo y se valida su funcionamiento.

Resultados— El algoritmo desarrollado e implementado en el prototipo desarrollado mitiga los fenómenos de calidad de la energía asociados a las variaciones de corta y larga duración como swell, sag, undervoltaje y overvoltaje, evita la presencia de fluctuaciones de tensión y presenta un contenido armónico menor en todos los casos del 1%

Conclusiones— El prototipo implementado optimizar la calidad de la energía de los sistemas trifásicos de suministro de energía a través del uso de un inversor multinivel, evitando la presencia de fenómenos de calidad de la energía.

Palabras clave— Algoritmo genético multiobjetivo; Convertidor multinivel; modulación por ancho de pulso; distorsión armónica total; calidad de la energía

Abstract

Introduction— The DC/AC conversion systems currently used in multiple applications such as alternative energy sources involve power quality problems due to voltage regulations and deformations such as those caused by harmonic distortion.

Objective— To develop a prototype that, through a multi-objective genetic algorithm, allows optimizing the energy quality of three-phase inversion systems through the use of multilevel converters.

Methodology— The prototype to be used in the power conversion is defined, the output voltage is modeled mathematically, the optimization multi-objective genetic algorithms are developed, the prototype is implemented and its operation is validated.

Results— The algorithm developed and implemented in the developed prototype mitigates the power quality phenomena associated with short and long duration variations such as swell, sag, undervoltage and overvoltage, avoids the presence of voltage fluctuations and presents a lower harmonic content, in all cases 1%

Conclusions— The implemented prototype optimizes the power quality of three-phase power supply systems through the use of a multilevel inverter, avoiding the presence of power quality phenomena.

Keywords— Multi-objective genetic algorithm; Multi-level converter; pulse width modulation; total harmonic distortion; power quality

I. INTRODUCTION

Nowadays the need to transform Direct Current to Alternating Current (DC/AC) in power converters is very recurrent, since this type of conversion is necessary in multiple applications, an example of this is photovoltaic systems that supply alternating loads or that are connected to the network, since the panels generate DC current but for the final use AC current is required [1], [2].

For this type of power conversion, it generally uses PWM modulation techniques, these techniques have been developed to a very high level [3], however, they present some drawbacks in terms of power quality and performance due to high rates of commutations that are generally used [4], [5]. A technique used in recent decades to improve waveforms, reduce the number of commutations and obtain a pure sinusoidal wave has been the use of multilevel power converters [6], [7], [8], devices that have their origin in the year of 1981 with the work of Japanese researchers who developed the first multilevel inverter [9], these devices allow to obtain staggered waves that are more similar to a sinusoidal wave with fewer commutations, these multilevel systems have presented a very good development in the last decades, allowing power inversion systems to reduce the harmonic content [10], [11].

In order to improve the waveforms, multiple investigations have been carried out in the field of harmonic optimization in these devices [12], [13], [14], proposing selective eliminations for specific harmonics or in special harmonic ranges [15], [16], [17], the ultimate goal is to completely eliminate harmonics, however this is still under development.

Similarly, in the field of power inversion, power quality problems are also associated with voltage fluctuations that may appear due to variations in the DC bus, in the case of photovoltaic systems, for the variation in the operating point of the panels, or in systems that use batteries due to the fluctuation in the voltage of the accumulator block [15], this can generate the appearance of short or long duration variations in the output of the inverters.

That is why this article presents the development of a power converter prototype that seeks to eliminate power quality problems in three-phase inversion systems using a multi-objective algorithm that seeks to find modulations applicable to a multilevel prototype, which has a waveform with optimum energy quality, but also involving a regulation system that allows the RMS level of the output waves to be kept constant, improving the energy quality of the DC/AC conversion systems.

II. METHODOLOGY

A. *Multilevel power converter*

In order to mitigate the power quality phenomena associated with the waveform in three-phase inversion systems, a multilevel power converter with 9 steps per phase and 17 steps per line is used. This number of levels guarantees that it can be reduce harmonic distortion with not-so-high switching, as will be shown in later sections. The line voltage has more steps than the phase voltage because the line voltage is generated by the potential difference of two phases, this subtraction generates more steps.

The multilevel converter selected was the cascaded H-bridge type, with a common source, so that the entire converter can be powered from a single source or DC bus, being attractive for DC/AC conversions from a single source. For this to happen, the transformers at the output of each stage will be in charge of adding the voltages of the H bridges and providing the galvanic insulation required to be able to add steps from the same sources.

The transformation ratios of the transformers used in each of the phases have an asymmetric ratio of 1:3, this in order that in each phase 9 steps can be obtained with only two H bridges, this configuration allows to have the maximum of steps with the minimum of stages.

To control the fluctuations that may exist in the output voltages of the multilevel converter, a small element DC/DC converter is implemented in the DC bus [17]. This converter allows with a minimum of elements to increase or reduce the voltage; In this way, connecting the direct current converter in cascade with the multilevel converter, a prototype capable of controlling the output voltage is obtained, by controlling the DC bus, and the inverter will be in charge of maintaining the characteristics of the waveform together with the desired frequency.

Due to the fact that the inverter generates a line voltage with more steps than the phase voltage, the commutations will not be as high, obtaining the minimum of harmonic distortion. The complete device topology is shown in Fig. 1 [16].

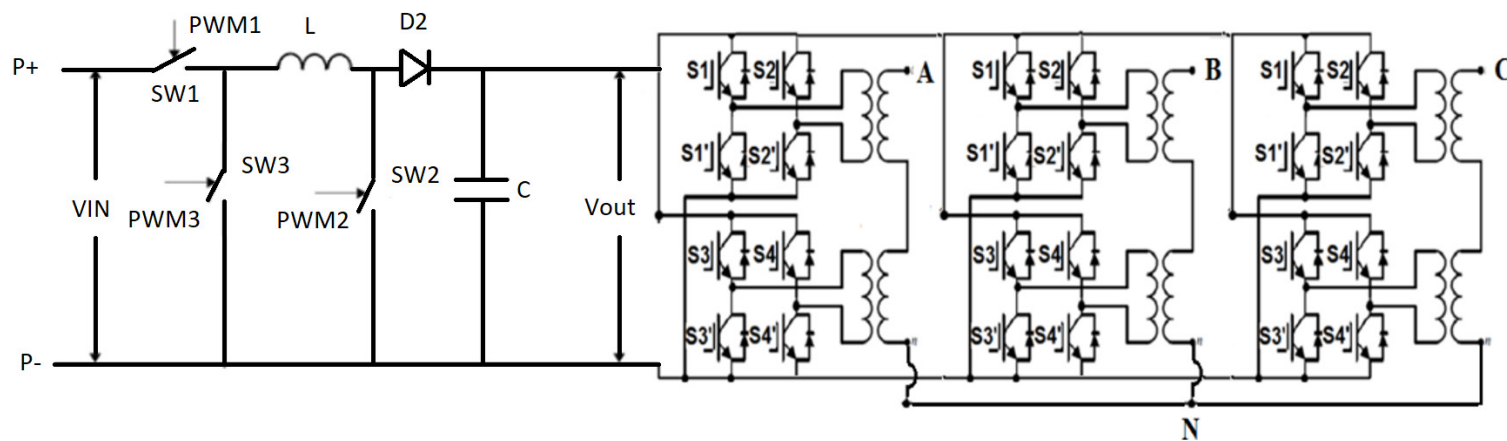


Fig. 1. Power converter topology.
Source: Authors.

B. Mathematical model

In order to generate an output waveform that has optimal energy quality, we start from the mathematical model of the harmonic content of a multilevel modulation (1). This model is based on the definition established by IEEE 519 (1992) of THD [19], [18].

$$THD = \frac{\sqrt{\sum_{n=2}^{50} h_n^2}}{h_1} \cdot 100 \quad (1)$$

Where h_n refers to the peak value of n harmonic.

The THD of the multilevel modulation is established in (2), this expression has been developed in previous works by the authors [13], [17].

$$THD = \frac{\sqrt{\sum_{n=2}^{50} \left(\frac{1}{n} \left[\sum_{i=1}^4 \sum_{j=1}^{L_i} (-1)^{j-1} \cos n \alpha_{ij} \right]^2 \right)}}{\left[\sum_{i=1}^4 \sum_{j=1}^{L_i} (-1)^{j-1} \cos 1 \alpha_{ij} \right]} * 100 \quad (2)$$

Where n takes odd values not multiples of 3, that is, 5, 7, 11, 13, etc. and L_i are the components of the vector $L = [a \ b \ c \ d]$, indicating the firing angles at each step of the first quarter wave of the phase modulation.

In the same way, to obtain a desired RMS level starting from the voltage given by the DC bus, equation 3 is established, which models the effective value of the multilevel modulation in terms of the DC voltage and the firing angles in each step, this expression has been developed in previous works by the authors.

$$V_{line_{RMS}} = \sqrt{\sum_{n=1}^{50} \frac{\left(\frac{4\sqrt{3} V_{dc}}{\pi n} \left[\sum_{i=1}^4 \sum_{j=1}^{L_i} (-1)^{j-1} \cos n \alpha_{ij} \right]^2 \right)}{2}} \quad (3)$$

para $n = 5, 7, 11, 13, \dots$

In this way, the waveform optimization problem is determined by (2), which defines the total harmonic distortion to be optimized, and (3) defines the effective value desired for the modulation. The optimization algorithm will receive the desired effective value and will look for a waveform that has the minimum expression of harmonics, but that is closest to the desired RMS value, modifying the switching angles in each of the modulation steps.

From the mathematical model it can be seen that harmonics that are multiples of three and even have no influence on the value of the THD or the value of the RMS voltage of the line modulation. This is because even harmonics do not exist due to the symmetry of the stepped waveform that can be obtained and harmonics that are multiples of three, being zero sequence, are subtracted from the phase difference when obtaining the line voltage.

C. Multi-objective optimization algorithm

With the aim of solving the multi-objective optimization problem, it was determined to use genetic algorithms as a tool to solve the problem. In Fig. 2 shows the flowchart of the multi-objective genetic algorithm developed to obtain a desired RMS value with the minimum THD value in the line voltage and with reduced commutations.

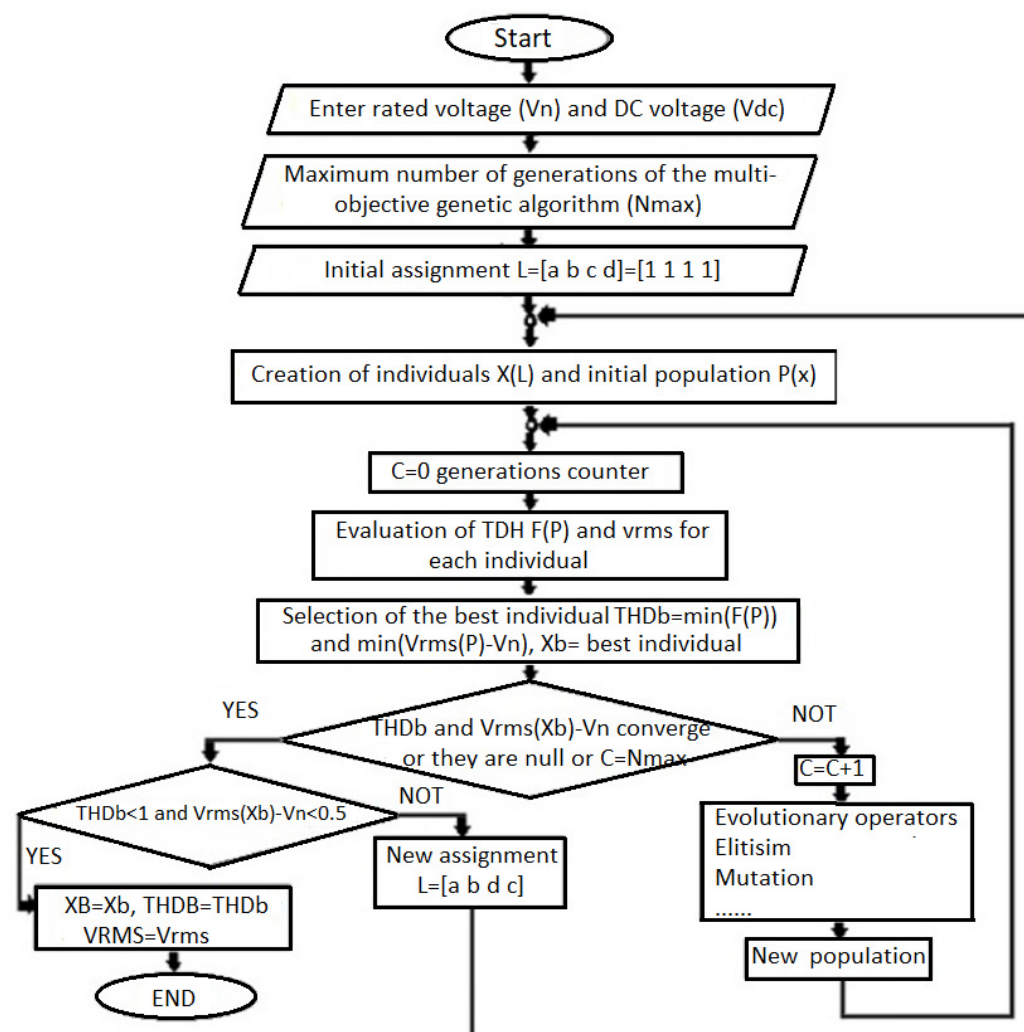


Fig. 2. Multiobjective genetic algorithm.
Source: Authors.

As input data, the desired rated line voltage and the value of the DC bus voltage are assigned, in the same way the maximum number of generations in which the algorithm can evolve per stage is indicated and an initial vector of the number of firing angles in each step of the first quarter wave of the phase modulation, so that it is the minimum possible, a vector of ones is assigned.

With this information, the algorithm creates an initial population where each individual has an initial angle in each step, evaluates the THD value for each individual and its RMS value, after which it selects the best individual and evaluates the convergence criteria of the generation, which are three: the first is that the maximum number of generations is exceeded, that the THD value is null and that the RMS value is the desired one. The third criterion is that the value of THD and VRMS converge.

If none of these criteria is met, the algorithm applies evolutionary operators such as mutation, elitism, among others, to create a new population and repeat the process. Once any of the convergence criteria is met, the algorithm evaluates if the data obtained from the best individual complies with the THD value being less than 1% and the RMS value of the line voltage being the desired value with a tolerance of 0.5 Volts.

If the conditions are not met, the algorithm will create a new vector of the number of shot angles by adding more shot angles. The evolution and evaluation process will be carried out again. In this way, if a satisfactory answer is not found, the algorithm will continue adding angles, until an individual is found that meets the conditions.

This logic allows finding a modulation that has a very low harmonic content, a desired voltage level, but with the minimum number of commutations required, contributing to the efficiency of the converter.

The described optimization algorithm was coded in Matlab® [21] using the multi-objective genetic algorithm toolbox. For the particular case of this research, the generated populations consisted of 20 individuals. The nominal values of the converter in terms of input voltage is 45 V, output 220 V line and a frequency of 60 Hz.

It should be noted that since the equations that determine the mathematical model are in the electrical angle domain, the output frequency will depend exclusively on the implementation, since the angles found must be converted to the time domain using the desired electrical frequency.

D. Implementation

The implemented power converter corresponds to the topology shown in Fig. 1. Its power source is a DC bus, which can correspond to a set of batteries. The converter integrates a 48V nominal reduced component variable DC/DC regulator and a 2400 VA three-phase multilevel DC/AC power inverter, at 60Hz with 127V and 220V line phase voltages regulated by the drive angles and the bus. of DC. The general scheme of the developed prototype powered by an autonomous PV system is shown in Fig. 3.

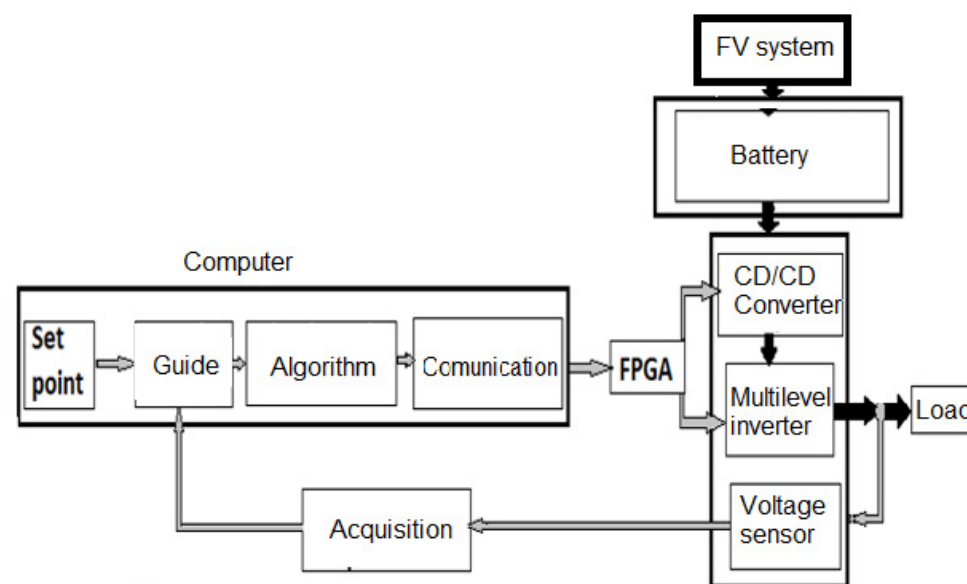


Fig. 3. Block diagram of the implemented power converter.
Source: Authors.

The control of the converter is carried out by means of a Virtex 5 FPGA board and the objective of this is to avoid the presence of events that deteriorate the quality of the energy, through the implementation of optimized drive angles based on the Total Harmonic Distortion (THD) and the RMS voltage, the effective value control is performed by controlling the variable DC/DC converter depending on the magnitude of the RMS voltage at the output of the prototype.

The verification and control of the DC/DC power converter was carried out in the Labview® [22] software, with the measurement of the AC RMS voltage as an input parameter to be compensated by means of a PID controller, for which this signal is acquired using a National DAQ 6009 card. Instrument, and the compensator constants are implemented in Labview®, sending the DC/DC converter control signal to the FPGA through the RS-232 protocol.

AC waveform enhancement is achieved by implementing a Genetic Algorithm (GA) that is performed offline. Developed based on the voltages for which the FPGA card replicates the switching angles through the control signals of the DC/AC converter. Fig. 4 shows a photo of the power converter.

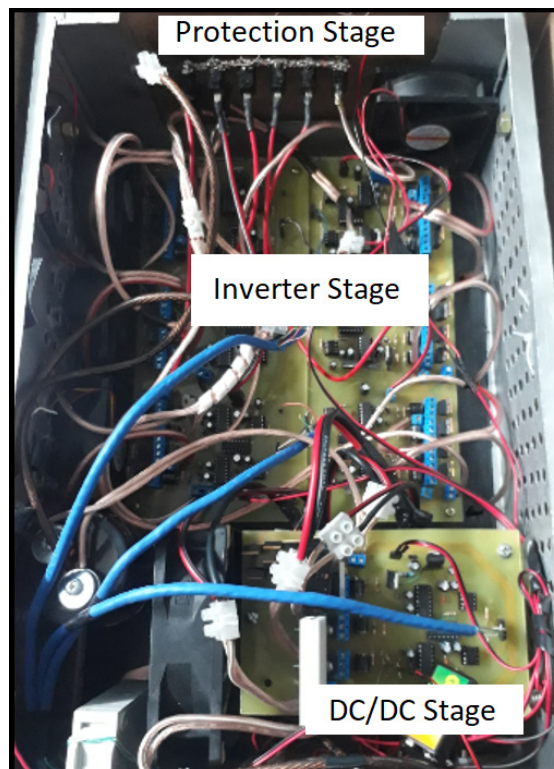


Fig. 4. Implementation of the power converter.
Source: Authors.

III. RESULTS AND DISCUSSION

The last evolution process of the optimization algorithm is presented in Fig. 5 where the behavior of the total harmonic distortion in the evaluated generations is evidenced. Through this, the 48 commutation angles obtained provide a THD value of 0.00006% with a line voltage of 219.99 V and a phase voltage of 127.011 V. The modulation consists of 5 switching angles in the first level, 7 in the second, 9 in the third and 27 in the fourth, represented in the vector $L = [5 \ 7 \ 9 \ 27]$. With a quarter wave symmetry modulation that eliminates even harmonics and the DC component.

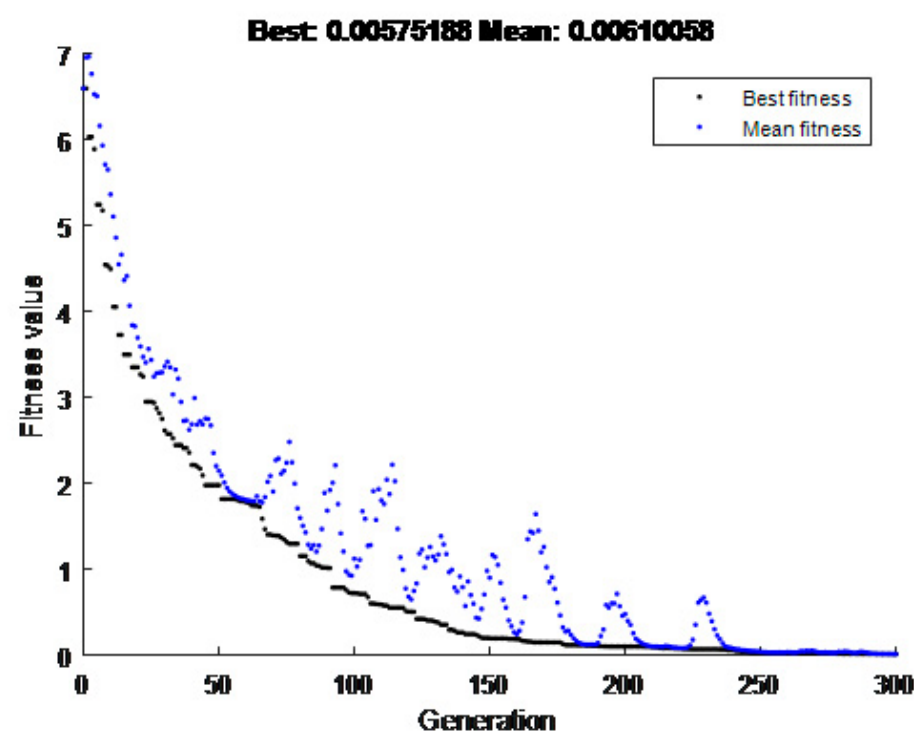


Fig. 5. Evolution of the algorithm in the last vector L .
Source: Authors.

The phase and line voltage waveforms are presented in Fig. 6 and Fig. 7. These show the increase in the number of levels in the line voltage. These better waveforms would be the ones delivered at the output of the power converter and would have modifiers of the magnitude of the DC bus that controls the RMS voltage.

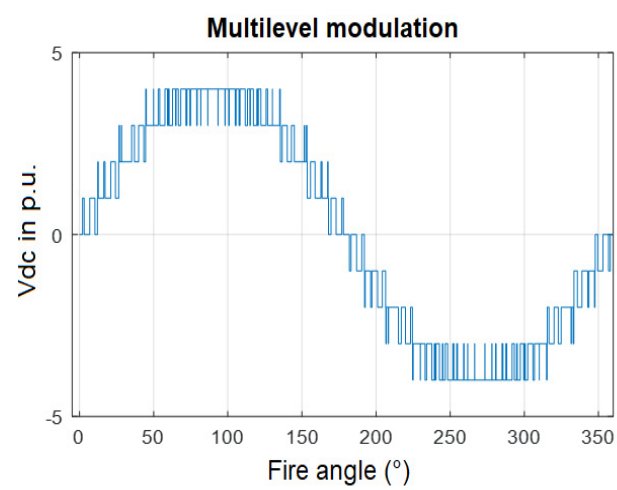


Fig. 6. Phase voltage waveforms.
Source: Authors.

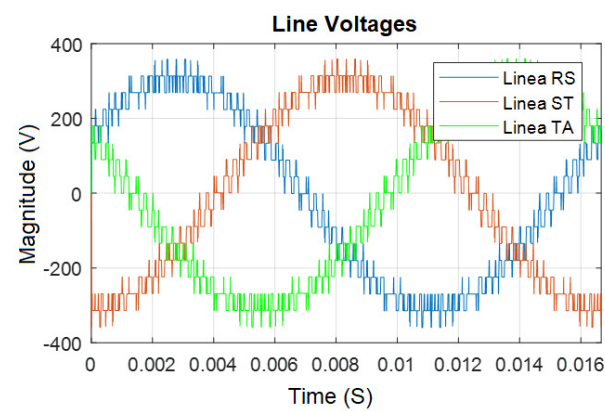


Fig. 7. Line voltage waveforms.
Source: Authors.

The harmonic spectra of these waveforms are practically zero since the harmonic content determined by the algorithm is 0.0006%. These harmonic spectra can be seen in Fig. 8 and Fig. 9. If these spectra are detailed, no contributions of any order are perceived in the first 50 harmonics. The line voltages, as they correspond to the subtraction of the phases, have 8 additional steps to the 9 phase steps. Which generates a cleaner spectrum, however, with the naked eye it is difficult to differentiate it from the phase spectrum, since both are practically zero.

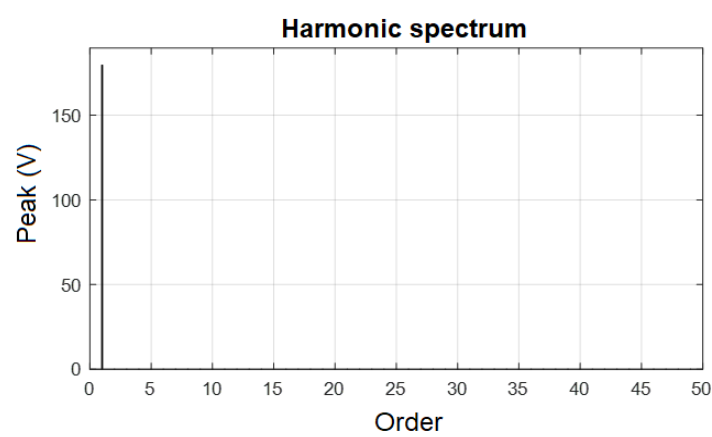


Fig. 8. Harmonic spectrum of the phase voltages.
Source: Authors.

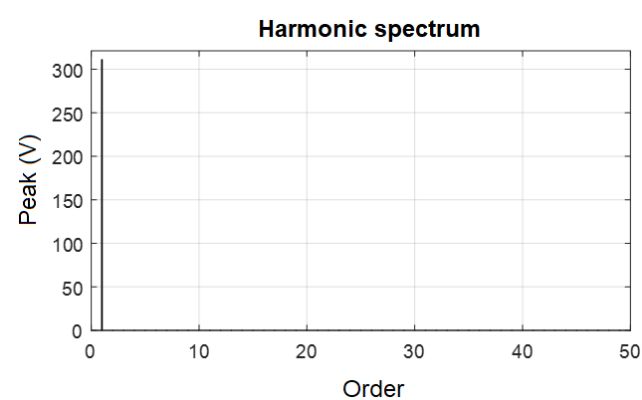


Fig. 9. Harmonic spectrum of line voltages.
Source: Authors.

Laboratory tests were carried out on the implemented prototype in order to validate its operation. This prototype was evaluated being applied to an autonomous photovoltaic system. The input of the power converter was fed from the accumulator block of the system and the output was connected to a three-phase charging system constituted by a three-phase rheostat. The test setup is shown in Fig. 10.

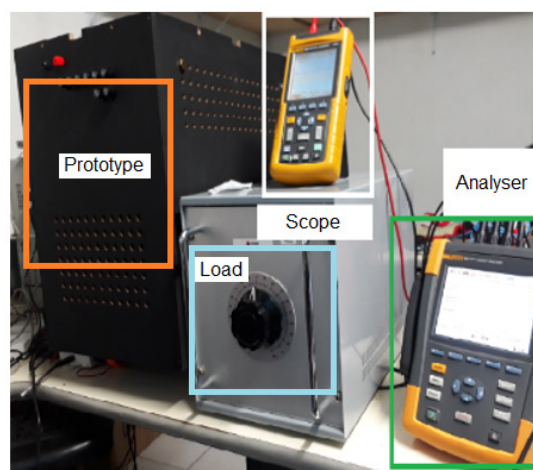


Fig. 10. Experimental setup.
Source: Authors.

The output and input variables of the prototype were measured, for this the Fluke 434 power quality analyzer was used. This in order to validate the power quality of the converter output, for the measurement of the variables of input, a data acquisition system based on the National Instruments NI USB 6211 card and the Fluke DP 120 voltage probe was used. In this way, the input and output variables are captured.

The developed test consisted in carrying out the deep discharge of the accumulator block of the photovoltaic system, through the supply of the three-phase rheostat through the prototype, variations were made in the rheostat in order to obtain load shots that could affect the output voltage. This is done in order to validate that the voltage level remains within the limits established by the IEEE 1159 [19] and IEEE 519 [20] standards.

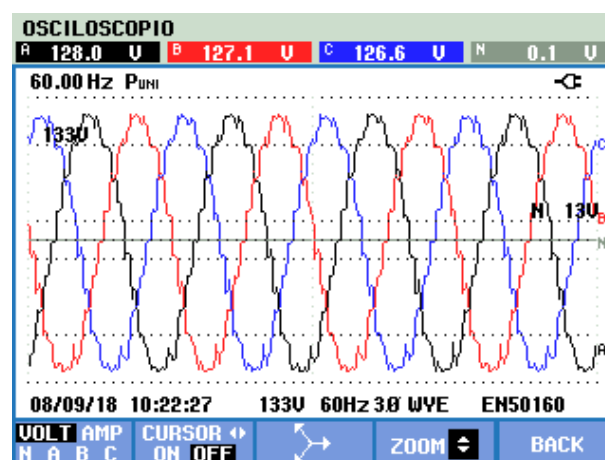


Fig. 11. Waveforms of the power converter phase voltage.
Source: Authors.

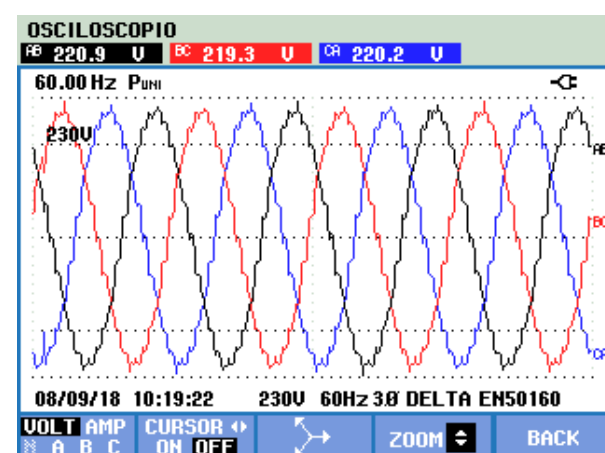


Fig. 12. Power converter line voltage waveforms.
Source: Authors.

The waveforms measured by the analyzer for the phase and line voltages are shown in Fig. 11 and Fig. 12 respectively.

In Fig. 11 some small differences are perceived between the effective values of phases A, B and C, these differences may be caused by some small constructive differences of the transformers, however, as will be shown later, the voltage unbalance is minimal and lower to 2%, which is suggested as typical in the IEEE 1159 standard [19]. In Fig. 12 shows that there are more steps in the line voltage than in the phase voltage, these waveforms are therefore visually closer to the pure sine wave.

Regarding the harmonic content of these waveforms, Fig. 13 and Fig. 14 present the spectra of the phase and line voltages respectively, the total harmonic distortion for the phase voltage is 0.8% and for the line voltage it is 0.5%, both values are very low, which complies with fully the suggestion of the IEEE 519 standard [18], where for low voltage systems it is suggested that the content be less than 8%.

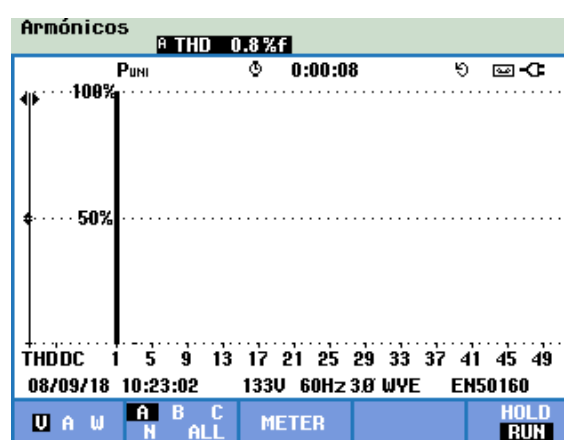


Fig. 13. Spectral content of the phase voltage.
Source: Authors.

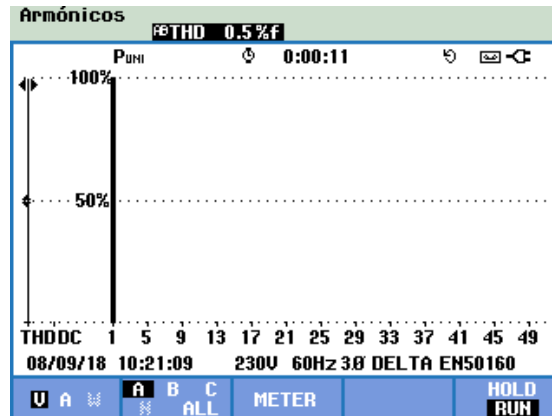


Fig. 14. Spectral content of the line voltage.
Source: Authors.

These measurements validate that the developed prototype generates a waveform with very low harmonic content, presenting good behavior in terms of spectral content and the absence of deformations.

Regarding the distortions present in the output currents of the power converter. In Fig. 15 shows their waveform and Fig. 16 its spectral content.

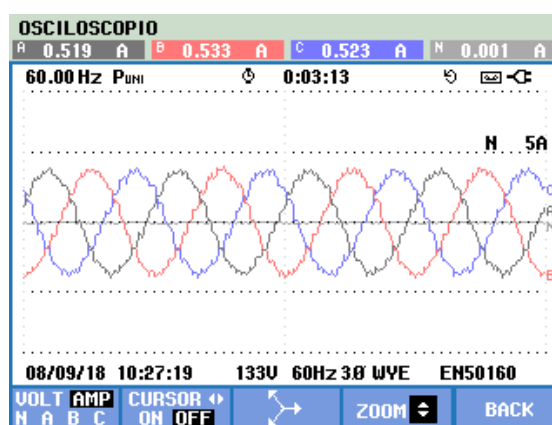


Fig. 15. Waveform of currents.
Source: Authors.

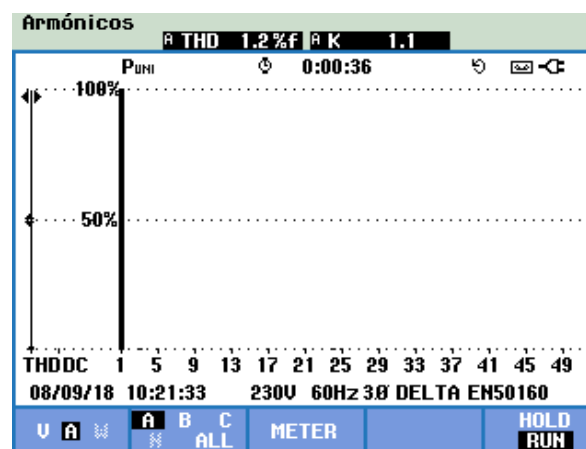


Fig. 16. Spectral content of currents.
Source: Authors.

The waveforms of the current are practically sinus waveforms, presenting an excellent behavior in the three waveforms of the lines (Fig. 15). As the power converter is star connected, the line and phase currents are equal and with a very low harmonic content, as shown in Fig. 16, there is practically no relevant contribution of harmonics. The current is characterized by a total harmonic distortion of only 1.2%, which is very good considering that the allowed harmonic contents in currents are wider than in voltages according to IEEE 519 [18].

With respect to three phase behavior, Fig. 17 shows the phasor diagrams of the currents and voltages, in these it is observed that the transformation system is balanced, presenting only small variations of less than 1 volt, this is due to differences between the transformers. However, the behavior is satisfactory since the voltage unbalance corresponds to a value less than 1%, more specifically it is 0.47% according to the ANSI methodology, which corresponds to excellent behavior since an acceptable unbalance must be less than two%.

Similarly, Fig. 17 presents the measured frequency, which is exactly 60 Hz, this validates that there will be no variations in the frequency, since the frequency is controlled by the control device that assigns the durations of the steps.

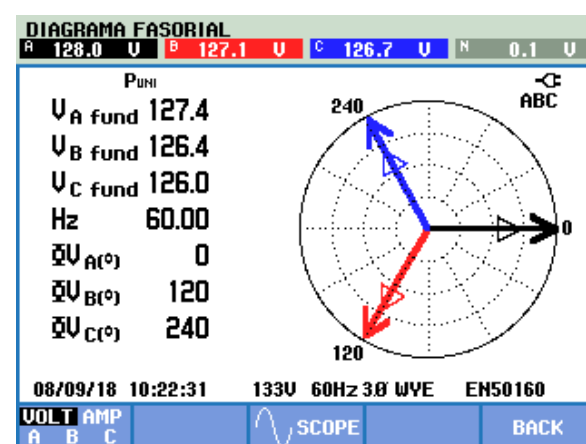


Fig. 17. Phasor diagrams of the measured variables.
Source: Authors.

The voltage profile of the power converter output and input are shown in Fig. 18a and Fig. 18b respectively. Drastic fluctuations in the input voltage can be observed, but when analyzing the output profile, the action of the proposed prototype is perceived since the RMS value of the output line voltage of the converter is flat. Presenting full compliance with the power quality requirements since the voltage level always remains between 0.9 p.u. and 1.1 in p.u. complying with power quality standards.

In detail, Fig. 18a shows the voltage profile of the converter output voltage, this profile is practically constant, due to the action of the regulation and optimization algorithm that allows maintaining a modulation with the desired value.

In Fig. 18b shows the profile of the input voltage of the converter, it is seen with strong variations due to the current demand of the load, and the current draw of the multilevel converter. It is also observed that the battery block voltage is initially higher than 50 volts and at the end of the test it is reduced to less than 43 volts, regardless of this behavior of the input voltage.

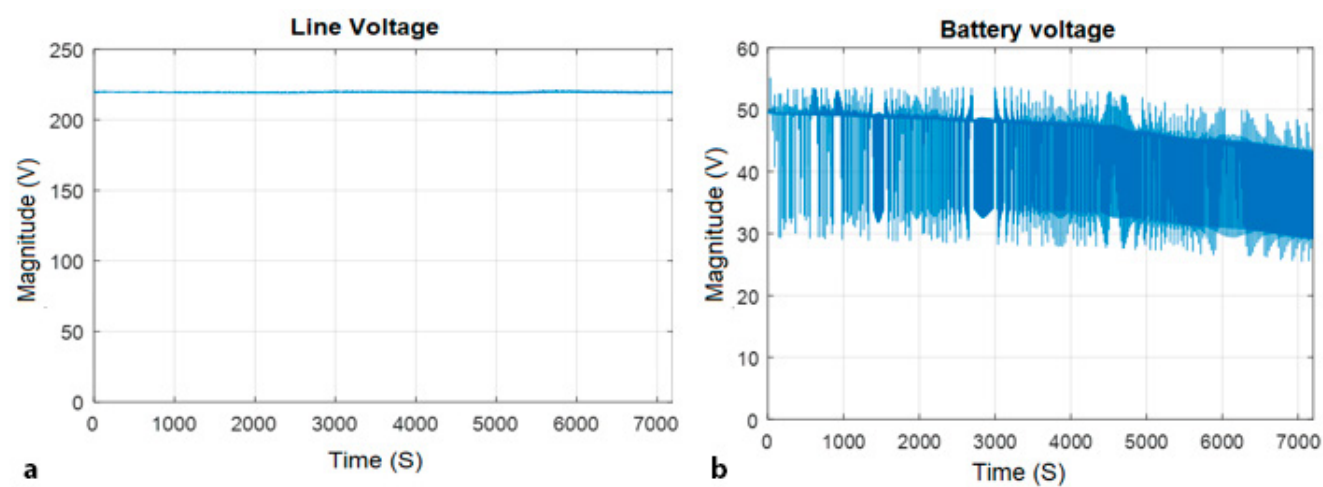


Fig. 18. a). RMS output voltage of the power converter; b). Input voltage.
Source: Authors.

At the output of the power converter, the voltage remains constant, which verifies that the prototype correctly mitigates the phenomena associated with long and short duration variations that could occur due to voltage variation, such as: swell, sag, undervoltage and overvoltage. Likewise, there are no flickers since the control of the output voltage prevents this phenomenon from occurring.

In Fig. 19 shows the extension of the output voltage profile, the maximum variation of the output voltage is less than one volt. This verifies the efficiency of the prototype in keeping the voltage constant, guaranteeing that regardless of raising or lowering the voltage on the DC bus, the output voltage will remain constant.

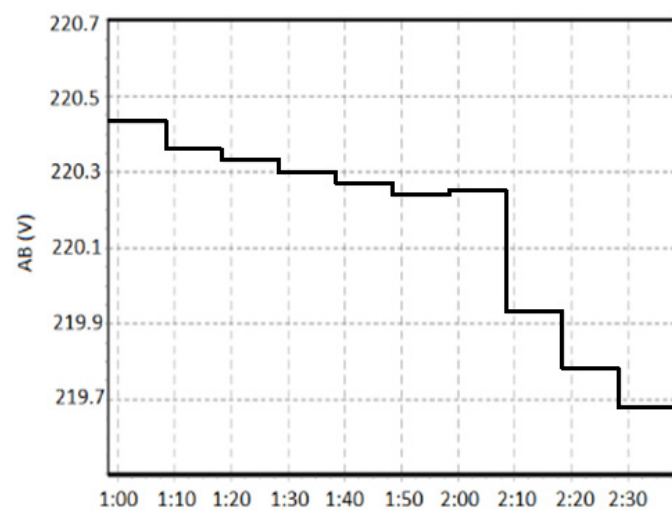


Fig. 19. a). Line RMS voltage; b). harmonic content.
Source: Authors.

The Fig. 20 allows validating the low order harmonic content, to be precise the first 25 harmonics, as well as the total harmonic distortion in the output voltage. The maximum measured value of harmonic distortion for the output voltage is 0.6% of the THD. Which allows us to say that the inverter has a pure sine waveform. The first 25 harmonics have negligible contents that are below 0.3%, as evidenced in that figure.

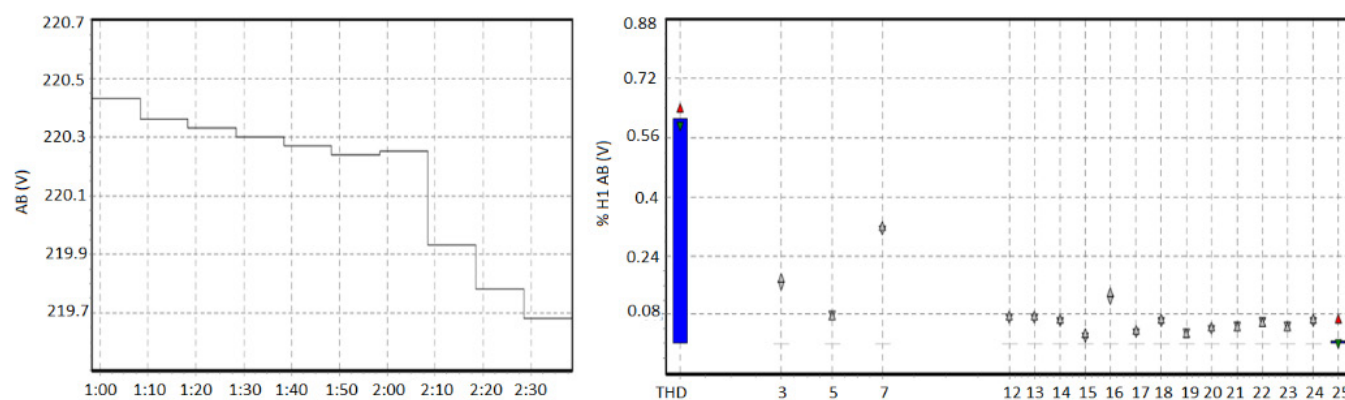


Fig. 20. a). Line RMS voltage; b). harmonic content.
Source: Authors.

In the tests carried out, there are no frequency variations or voltage imbalances. These phenomena are mitigated by the developed prototype thanks to the implementation and regulation algorithms. The Fig. 21 shows the evaluation for these phenomena delivered by the network analyzer.

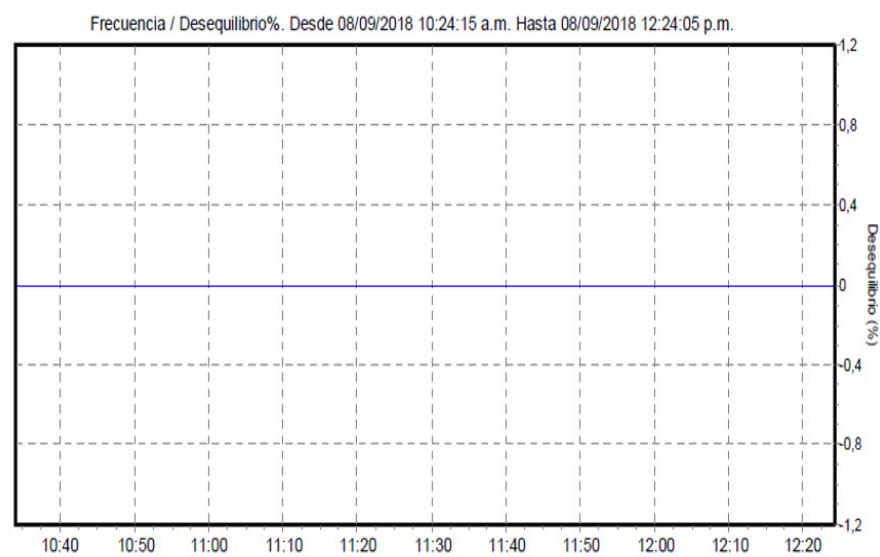


Fig. 21. Voltage imbalances and frequency variations.
Source: Authors.

Within the total evaluation of the quality of the power, it can be established that there were no events, regardless of the discharge of the accumulator block and the variations in the load, this validates the operation of the proposed prototype.

Finally, it should be noted that the transient phenomena have not been verified since the network analyzer used does not allow the evaluation of transient phenomena, therefore, the evaluation of this category of power quality phenomena is left for future work.

In the same way, it is highlighted that as for the contrast of the improvement made in this project with respect to the classical optimization techniques, the algorithm used gives a purely numerical character to the harmonic optimization problem, since by not using comparisons of modulated and modulating waves and treating each firing angle as an independent variable, the THD indicators can practically be completely annulled improving the results obtained with classical optimization techniques where sine waves are compared with triangular waves, sawtooth, etc. However, this also implies that real-time optimization operation is very difficult to achieve, so the technique used will be an off-line technique.

Regarding the evaluation of transient phenomena, it is necessary to continue the research in future works where it is important to develop transient tests and analyze the results by comparing the transient response where the proposal is contrasted with classical control techniques and thus determine whether the calculation times of the algorithm to changes in operating conditions of the equipment are adequate for its implementation.

IV. CONCLUSIONS

Once the results obtained from the validation of the power quality test have been analyzed, it is established that the developed prototype allows the elimination of power quality phenomena associated with short and long duration variations such as sag, swell, undervoltage, overvoltage, etc. in the same way, if the application involves an accumulator block, it will allow to eliminate the interruptions; and as for the waveform, it reduces the phenomena associated with harmonic distortion, interharmonics, subharmonics and the DC component, it also mitigates frequency deviations and the presence of unbalances, due to the control loop implemented, the presence of flicker is also avoided.

The harmonic distortion optimization algorithm allows to determine with great precision the firing angles required to obtain a minimum of distortion, with a desired RMS value, as it could be observed in the tests carried out, all the harmonic contents were below the range of 1%, reaching experimental values of 0.6%, which validates the excellent result in terms of harmonics.

The regulation proposed in the DC bus carried out through the small element converter presented an excellent behavior by allowing the output voltage to remain constant regardless of the possible fluctuations in the input source or the load shocks and variations generated in the load.

The way in which the algorithm modifies the number of firing angles in each step allows the optimization to be carried out with a reduced number of commutations, since the algorithm starts with the smallest number and increases until it finds the required optimization. This contributes to increased efficiency by reducing switching losses.

The proposed topology has an advantage since the multilevel converter is star-connected, and the inverter can supply three-phase energy with only two phases, since the transformers could operate as an open delta.

FINANCING

This scientific research article is derived from work associated with the project “Ferro-resonant energy conditioner for photovoltaic systems”, which was financed by the University of Pamplona in the period 2020-2021.

ACKNOWLEDGMENTS

Special thanks to the University of Pamplona for the support received in carrying out the project whose activities and partial results allowed the preparation of this work.

REFERENCES

- [1] S. Deshpande & N. R. Bhasme, “A review of topologies of inverter for grid connected PV systems,” presented at the *2017 Innovations in Power and Advanced Computing Technologies*, i-PACT, VOVR, IN, Sept. 21-22, 2017. <https://doi.org/10.1109/IPACT.2017.8245191>
- [2] D. Barater, E. Lorenzani, C. Concari, G. Franceschini & G. Buticchi, “Recent advances in single-phase transformerless photovoltaic inverters,” *IET Renew Power Gener*, vol. 10, no. 2, pp. 260–273, Feb. 2016. <https://doi.org/10.1049/iet-rpg.2015.0101>
- [3] V. Gaikwad, S. Mutha, R. Mundhe, O. Sagar & T. Chinchole, “Survey of PWM techniques for solar inverter,” presented at the *2016 International Conference on Global Trends in Signal Processing, Information Computing and Communication*, ICGTSPICC, JVL, IN, Dec. 22-24, 2016. <https://doi.org/10.1109/ICGTSPICC.2016.7955352>
- [4] S. A. Saleh & M. A. Rahman, “Modeling of Power Inverters,” in *An Introduction to Wavelet Modulated Inverters*, NY, USA: Wiley-IEEE Press, 2011, pp. 41–63. <https://doi.org/10.1002/9780470647998.ch3>
- [5] S. A. Saleh & M. A. Rahman, “Introduction to Power Inverters,” in *An Introduction to Wavelet Modulated Inverters*, NY, USA: Wiley-IEEE Press, 2011, pp. 1–17. <https://doi.org/10.1002/9780470647998.ch1>
- [6] A. Ruderman, “About Voltage Total Harmonic Distortion for Single- and Three-Phase Multilevel Inverters,” *IEEE Trans Ind Electron*, vol. 62, no. 3, pp. 1548–1551, Mar. 2015. <https://doi.org/10.1109/TIE.2014.2341557>
- [7] B. Wu & M. Narimani, “Other Multilevel Voltage Source Inverters,” in *High-Power Converters and AC Drives*, NY-USA: Wiley-IEEE Pres, 2016, pp. 185–223. <https://doi.org/10.1002/9781119156079.ch9>
- [8] H. Abu-Rub, M. Malinowski & K. Al-Haddad, “Multilevel Converter/Inverter Topologies and Applications,” in *Power Electronics for Renewable Energy Systems, Transportation and Industrial Applications*, NY-USA: Wiley-IEEE Pres, 2014, pp. 442-462.
- [9] A. Nabae, I. Takahashi & H. Akagi, “A New Neutral-Point-Clamped PWM Inverter,” *IEEE Trans Ind Appl*, vol. IA-17, no. 5, pp. 518–523, Sep. 1981. <https://doi.org/10.1109/TIA.1981.4503992>
- [10] A. K. Koshti & M. N. Rao, “A brief review on multilevel inverter topologies,” presented at the *2017 International Conference on Data Management, Analytics and Innovation*, ICDMAI, PNQ, IN, Feb. 24-26, 2017. <https://doi.org/10.1109/ICDMAI.2017.8073508>
- [11] V. Roberge, M. Tarbouchi & F. Okou, “Strategies to Accelerate Harmonic Minimization in Multilevel Inverters Using a Parallel Genetic Algorithm on Graphical Processing Unit,” *IEEE Trans Power Electron*, vol. 29, no. 10, pp. 5087–5090, Oct. 2014. <https://doi.org/10.1109/TPEL.2014.2311737>
- [12] G. Ghosh, S. Sarkar, S. Mukherjee, T. Pal & S. Sen, “A comparative study of different multilevel inverters,” presented at the *2017 1st International Conference on Electronics, Materials Engineering and Nano-Technology*, IEMENTech, KMA, IN, Apr. 28-29, 2017. <https://doi.org/10.1109/IEMENTECH.2017.8076971>
- [13] T. Jacob & L. P. Suresh, “A review paper on the elimination of harmonics in multilevel inverters using bioinspired algorithms,” presented at the *2016 International Conference on Circuit, Power and Computing Technologies*, ICCPCT, NGL, IN, Mar. 18-19, 2016. <https://doi.org/10.1109/ICCPCT.2016.7530273>
- [14] M. Srndovic, A. Zhetessov, T. Alizadeh, Y. L. Familiant, G. Grandi & A. Ruderman, “Simultaneous Selective Harmonic Elimination and THD Minimization for a Single-Phase Multilevel Inverter With Staircase Modulation,” *IEEE Trans Ind Appl*, vol. 54, no. 2, pp. 1532–1541, Mar. 2018. <https://doi.org/10.1109/TIA.2017.2775178>

- [15] A. Anurag, N. Deshmukh, A. Maguluri & S. Anand, “Integrated DC–DC Converter Based Grid-Connected Transformerless Photovoltaic Inverter with Extended Input Voltage Range,” *IEEE Trans Power Electron*, vol. 33, no. 10, pp. 8322–8330, Oct. 2018. <https://doi.org/10.1109/TPEL.2017.2779144>
- [16] L. D. Pabón, J. L. Díaz & E. A. Caicedo, “Optimization of the THD and the RMS voltage of a cascaded multilevel power converter,” presented at the *2018 IEEE International Conference on Automation/XXIII Congress of the Chilean Association of Automatic Control*, ICA-ACCA, CCP, CL, Oct. 17-19, 2018. <https://doi.org/10.1109/ICA-ACCA.2018.8609770>
- [17] L. D. Pabón, J. L. Díaz & E. A. Arévalo, “Multilevel power converter with variable frequency and low constant total harmonic distortion,” presented at the *2014 IEEE 5th Colombian Workshop on Circuits and Systems*, CWCAS, BO, CO, Oct. 16-17, 2014. <https://doi.org/10.1109/CWCAS.2014.6994600>
- [18] R. S. Weissbach & K. M. Torres, “A noninverting buck-boost converter with reduced components using a microcontroller,” presented at the *IEEE SoutheastCon 2001*, Cat. No.01CH37208, Clemson, SC, USA, Apr. 1, 2001. <https://doi.org/10.1109/SECON.2001.923091>
- [19] *IEEE Recommended Practice and Requirements for Harmonic Control in Electric Power Systems*, IEEE 519-1992, IEEE, Institute of Electrical and Electronics Engineers, NJ, USA, 1992. Available: <https://standards.ieee.org/ieee/519/764/>
- [20] *IEEE Recommended Practice for Monitoring Electric Power Quality*, IEEE 1159-1995, IEEE, Institute of Electrical and Electronics Engineers, NJ, USA, 1995. Available: <https://standards.ieee.org/ieee/1159/1760/>
- [21] *Matlab*. (9.1). MathWorks, 2016. Available: <https://www.mathworks.com/products/matlab.html>
- [22] *Labview*. (2010). Engineer Ambitiously, 2010. Available: <https://www.ni.com/es-mx/shop/labview.html>

Jorge Luis Díaz Rodríguez. Universidad de Pamplona (Pamplona, Colombia). <https://orcid.org/0000-0001-7661-8665>

Luis David Pavón Fernández. Universidad de Pamplona (Pamplona, Colombia). <https://orcid.org/0000-0003-1788-4781>

Edison Andrés Caicedo Peñaranda. Universidad de Pamplona (Pamplona, Colombia). <https://orcid.org/0000-0003-4557-1061>